

Electronic Supplementary Information (ESI)

2D-to-disguised 3D materials with built-in acid sites: H⁺-[Al]-RUB-18

Francisca S. O. Ramos¹, Heloise O. Pastore^{1*}

Micro and Mesoporous Molecular Sieves Group, Institute of Chemistry, University of Campinas, 270,
Monteiro Lobato St., University Campus, Campinas, 13083-862, SP, Brazil.

* Corresponding Author: gpmmm@iqm.unicamp.br

Figure S1. Thermogravimetry (A) and its derivative (B) of the (a) Na-R18, (b) Na-[Al15_22]-R18, (c) Na-[Al30_42]-R18, and (d) Na-[Al60_40]-R18.

Figure S2. Thermogravimetry (A) and its derivative (B) of (a) CTA-R18, (b) CTA-[Al15_22]-R18, (c) CTA-[Al30_42]-R18, and (d) CTA-[Al60_40]-R18.

Figure S3. Powder XRD patterns of (a) CTA-RUB-18, (b) CTA-[Al15_22]-R18, (c) CTA-[Al30_42]-R18 and (d) CTA-[Al60_40]-R18.

Figure S4. Powder XRD patterns of the as synthesized pillared materials (a) R18-pil, (b) [Al22_41]-R18-pil, (c) [Al42_66]-R18-pil and (d) [Al40_131]-R18-pil.

Figure S5. ²⁷Al NMR spectra of (a) CTA-[Al15_22]-R18, (b) CTA-[Al30_42] and (c) CTA-[Al60_40]-R18.

Figure S6. ²⁷Al NMR spectra of (a) [Al22_41]-R18-pil, (b) [Al42_66]-R18-pil and (c) [Al40_131]-R18-pil.

Figure S7. ²⁹Si NMR spectra of (a) CTA-R18, (b) CTA-[Al15_22]-R18, (c) CTA-[Al30_42]-R18, and(d) CTA-[Al60_40]-R18.

Figure S8. ²⁹Si NMR spectra of (a) [Al22_41]-R18-pil, (b) [Al42_66]-R18-pil and (c) [Al40_131]-R18-pil.

Table S1. Empirical Formula of the Na-[Al]-RUB-18 aluminosilicates prepared through ICP OES and TGA data.

Table S2. Chemical Analysis of the samples exchanged with CTA⁺ ions, CTA⁺/unit cell and ion exchange degree for each sample.

Unit Cell Determination

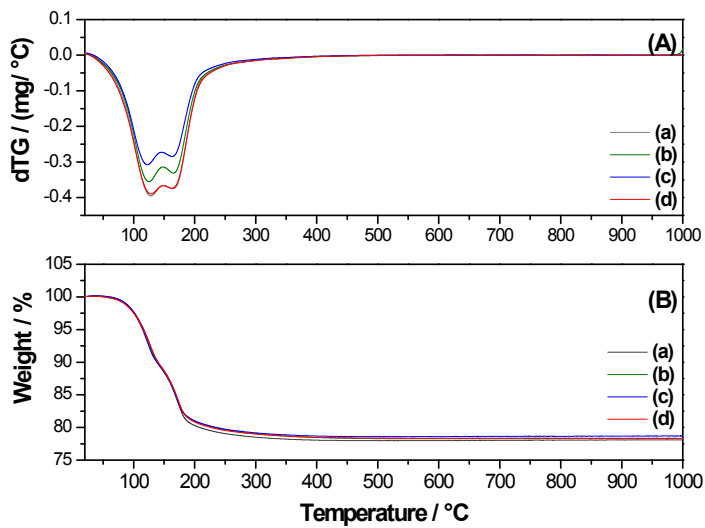


Figure S1. Thermogravimetry (A) and its derivative (B) of the (a) Na-R18, (b) Na-[Al15_22]-R18, (c) Na-[Al30_42]-R18, and (d) Na-[Al60_40]-R18.

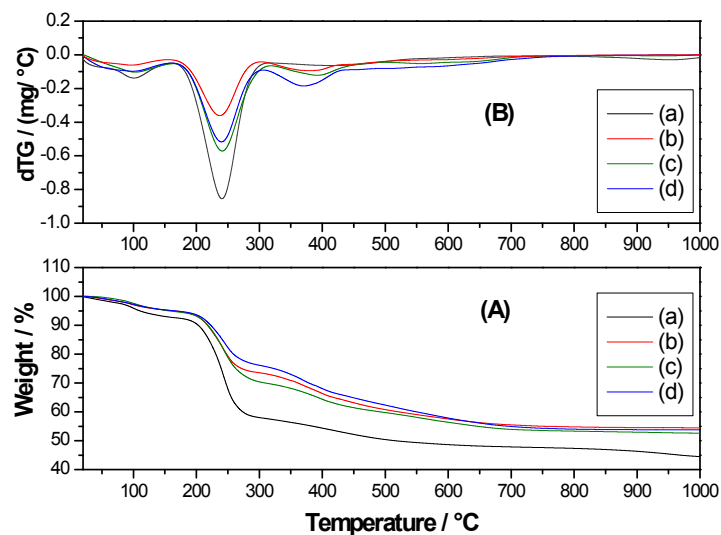


Figure S2. Thermogravimetry (A) and its derivative (B) of (a) CTA-R18, (b) CTA-[Al15_22]-R18, (c) CTA-[Al30_42]-R18, and (d) CTA-[Al60_40]-R18.

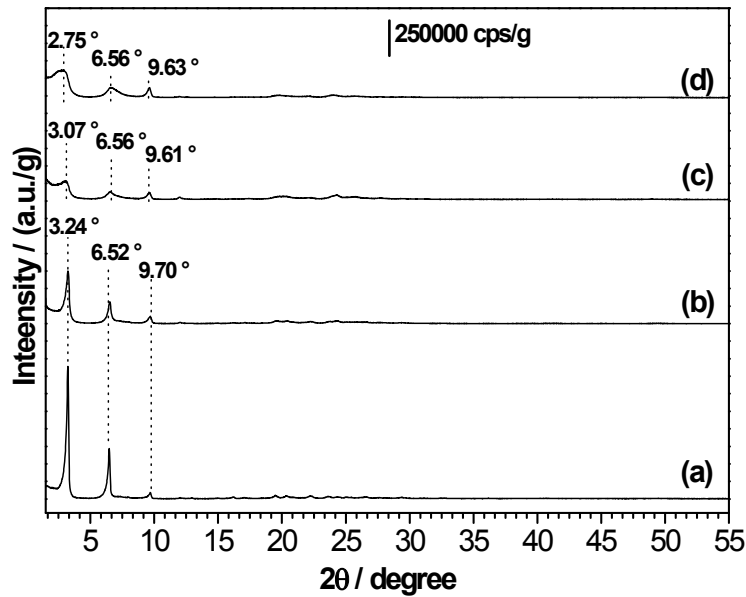


Figure S3. Powder XRD patterns of (a) CTA-RUB-18, (b) CTA-[Al15_22]-R18, (c) CTA-[Al30_42]-R18 and (d) CTA-[Al60_40]-R18.

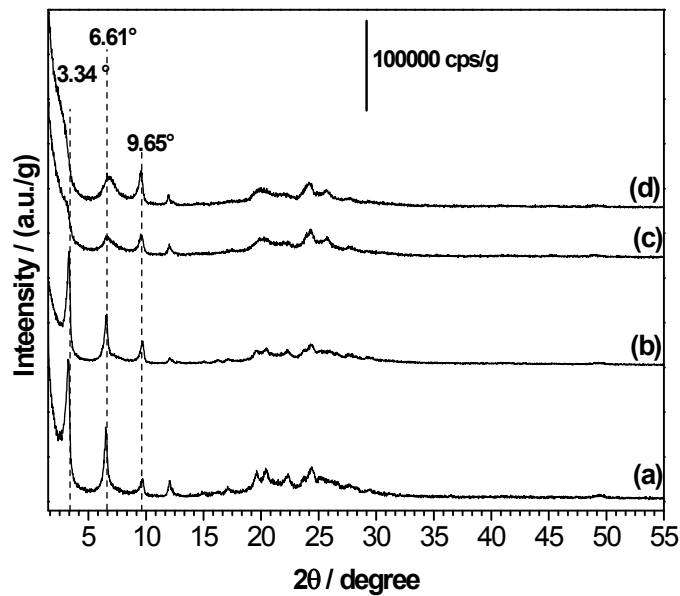


Figure S4 Powder XRD patterns of the as synthesized pillared materials (a) R18-pil, (b) [Al15_22]-R18-pil, (c) [Al30_42]-R18-pil and (d) [Al60_40]-R18-pil.

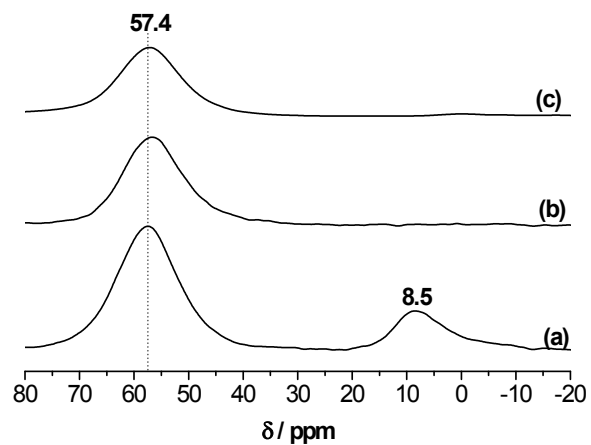


Figure S5. ^{27}Al NMR spectra of (a) CTA-[Al15_22]-R18, (b) CTA-[Al30_42]-R18 and (c) CTA-[Al60_40]-R18.

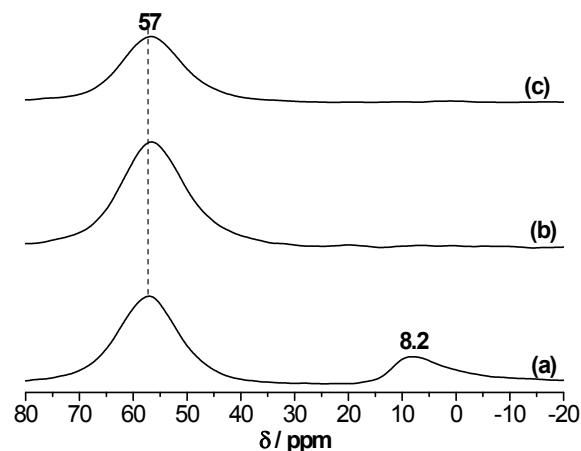


Figure S6. ^{27}Al NMR spectra of (a) [Al15_22]-R18-pil, (b) [Al30_42]-R18-pil and (c) [Al60_40]-R18-pil.

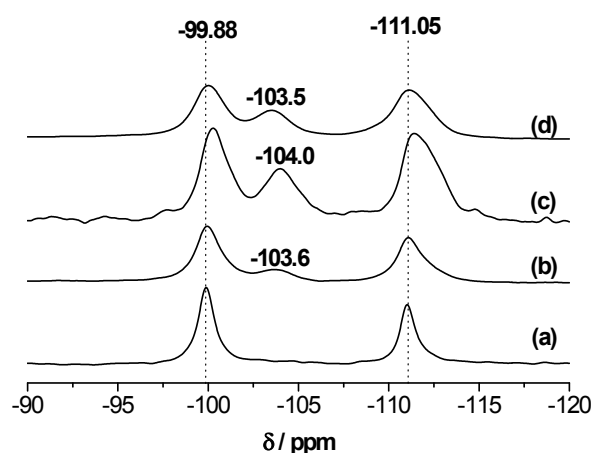


Figure S7. ^{29}Si NMR spectra of (a) CTA-R18, (b) CTA-[Al15_22]-R18, (c) CTA-[Al30_42]-R18, and(d) CTA-[Al60_40]-R18.

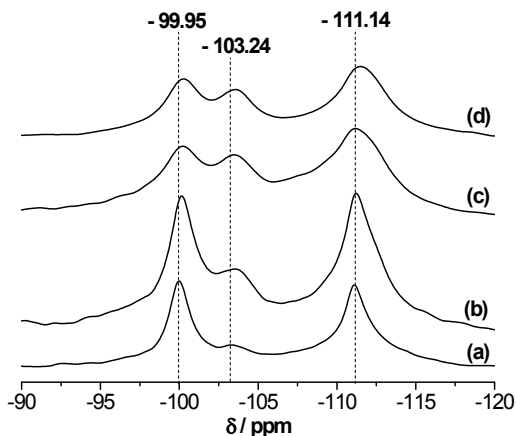


Figure S8. ^{29}Si NMR spectra of (a) [Al15_22]-R18-pil, (b) [Al30_42]-R18-pil and (c) [Al60_40]-R18-pil.

Table S1. Empirical Formula of the Na-[Al]-RUB-18 aluminosilicates prepared through ICP OES and TGA data.

Sample	Empirical Formula
Na-[Al15_22]-R18	$\text{Na}_{7,4}[\text{Si}_{30,63}\text{Al}_{1,37}\text{O}_{64}(\text{OH})_8] \cdot 25\text{H}_2\text{O}$
Na-[Al30_42]-R18	$\text{Na}_{8,1}[\text{Si}_{31,25}\text{Al}_{0,75}\text{O}_{64}(\text{OH})_8] \cdot 24\text{H}_2\text{O}$
Na-[Al60_40]-R18	$\text{Na}_{9,8}[\text{Si}_{31,22}\text{Al}_{0,78}\text{O}_{64}(\text{OH})_8] \cdot 26\text{H}_2\text{O}$

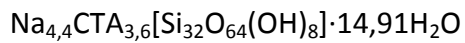
Table S2. Chemical Analysis of the samples exchanged with CTA⁺ ions, CTA⁺/unit cell and ion exchange degree for each sample.

CTA-sample	C / %*	N / %*	H / %*	CTA / mol	Ion Exchange degree / % ^a
CTA-R18	35.20	1.63	6.79	3.5	45
CTA-[Al15_22]-R18	31.02	1.43	6.71	3.2	42
CTA-[Al30_42]-R18	28.87	1.19	6.27	3.1	38
CTA-[Al60_40]-R18	21.15	1.04	6.07	3.0	31

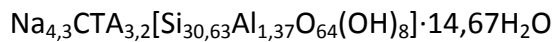
*% = m/m; ^a100% = all Na⁺ ions were replaced by CTA⁺ ions

Unit cells calculated from CHN (Table S1) and TGA (Fig S1):

▪ **CTA-RUB-18:**



▪ **CTA-[Al15_22]RUB-18:**



▪ **CTA-[Al30_42]RUB-18:**



▪ **CTA-[Al60_40]RUB-18:**

